CHEMISTRY

Hydrogen-bond donor and acceptor cooperative catalysis strategy for cyclic dehydration of diols to access O-heterocycles

Huan Wang[1,2], Yanfei Zhao[1,2], Fengtao Zhang[1,2], Zhengang Ke[1], Buxing Han[1,2,3], Junfeng Xiang[4], Zhenpeng Wang[4], Zhimin Liu[1,2,3]*

Dehydrative cyclization of diols to O-heterocycles is attractive, but acid and/or metal-based catalysts are generally required. Here, we present a hydrogen-bond donor and acceptor cooperative catalysis strategy for the synthesis of O-heterocycles from diols in ionic liquids [ILs; e.g., 1-hydroxyethyl-3-methyl imidazolium trifluoromethanesulfonate ([HO-EtMIm][OTf])] under metal-free, acid-free, and mild conditions. [HO-EtMIm][OTf] is tolerant to a wide diol scope, shows performance even better than H_2SO_4, and affords a series of O-heterocycles including tetrahydrofurans, tetrahydropyrans, morpholines, dioxanes, and thioxane in high yields. Mechanism investigation indicates that the IL cation and anion serve as hydrogen-bond donor and acceptor, respectively, to activate the C—O and O—H bonds of alcohol via hydrogen bonds, which synergistically catalyze dehydrative cyclization of diols to O-heterocycles. Notably, the products could be spontaneously separated after reaction because of their immiscibility with the IL, and the IL could be recycled. This green strategy has great potential for application in industry.

INTRODUCTION

O-heterocycles such as tetrahydrofurans, tetrahydropyrans, morpholines, dioxanes, and thioxane are essential chemicals with wide applications such as solvents, environmentally friendly alternative fuels for diesel engines, pharmaceuticals, intermediates for fine chemicals, and so on, and they are mainly produced via dehydrative cyclization of diols over acidic catalytic systems (Fig. 1) (*1*–*6*). Homogeneously catalytic systems including Brønsted acids (e.g., H_2SO_4, H_3PO_4, and H_3PO_2), Lewis acids [e.g., $BuSnCl_3$, $CuBr_2$, and $Fe(OTf)_3$], and metal-based complex catalysts (e.g., Ru/P/Al) have been widely applied in catalyzing dehydrative cyclization of diols to access cyclic ethers (*5*, *7*–*9*). However, they generally suffer from corrosion, pollution, and difficulty in separation, thus limiting their practical applications (*10*–*15*). Heterogeneous catalysts with high performances and stability, including solid-acid catalysts (e.g., γ-Al_2O_3, H-ZSM-5, H-Y, and H-ZSM-22) and solid-metal complexes (e.g., NHC-Ir), have also been intensively applied in the dehydrative cyclization of diols, which require high temperature (e.g., 200° to 400°C), leading to the formation of by-products (e.g., hydrocarbons and coke) and deactivation of catalysts (*11*, *16*–*19*). To date, efficient synthesis of O-heterocycles via dehydrative cyclization of diols in a green and mild way remains challenging. Therefore, developing simple and green approaches together with a previously unidentified reaction mechanism is highly desirable.

Hydrogen bond interaction is widely present in nature (*20*–*22*), and hydrogen bond catalysis is an efficient way to achieve chemical transformation under metal-free conditions (*23*–*25*). Ionic liquids (ILs) are totally composed of organic cations and organic or inorganic anions, in which strong hydrogen-bond interactions exist between ionic and molecular/ionic species because of the presence of electrostatic forces (*26*–*28*). The unique hydrogen bond interaction of ILs is capable of catalyzing the chemical reactions under metal-free and mild conditions (*29*, *30*), showing promising applications in catalysis. For example, various CO_2-philic ILs could activate substrates via hydrogen-bond interaction, thus promoting the reaction of CO_2 with the substrates under metal-free conditions (*31*, *32*).

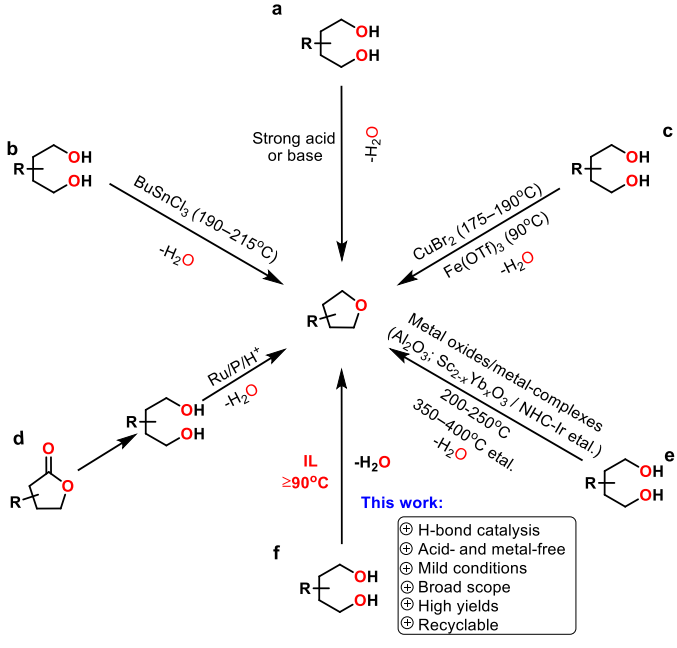

Fig. 1. Reaction development for dehydrative cyclization of diols.

[1]Beijing National Laboratory for Molecular Sciences, Key Laboratory of Colloid and Interface and Thermodynamics, CAS Research/Education Center for Excellence in Molecular Sciences, Institute of Chemistry, Chinese Academy of Sciences, Beijing, P. R. China. [2]University of Chinese Academy of Sciences, Beijing 100049, P. R. China. [3]Physical Science Laboratory, Huairou National Comprehensive Science Center, Beijing 101400, P. R. China. [4]Center for Physicochemical Analysis and Measurement, Institute of Chemistry, Chinese Academy of Sciences, Beijing 100190, P. R. China.
*Corresponding author. Email: liuzm@iccas.ac.cn

Basic IL 1-ethyl-3-methylimidazolium acetate ([EMIM][OAc]) could efficiently catalyze one-pot oxidative transformation of alcohols into esters by hydrogen bond (*29*). The imidazolium ILs functionalized with -SO_3H could catalyze the ring-closing metathesis of aliphatic ethers through three strong hydrogen bonds (*30*). Obviously, the hydrogen bond interactions in IL systems play important roles in these reactions. However, the mechanism of hydrogen bond catalysis is still ambiguous, and hydrogen bond–catalyzed dehydration of alcohols has not been reported in a literature survey.

In this work, we present a promising strategy for the synthesis of O-heterocycles from diols in ILs, e.g., 1-hydroxyethyl-3-methyl imidazolium trifluoromethanesulfonate ([HO-EtMIm][OTf]), under metal-free, acid-free, and mild conditions (≥90°C). It was indicated that [HO-EtMIm][OTf] was tolerant to a wide diol scope, and a series of O-heterocycles including tetrahydrofurans, tetrahydropyrans, morpholines, dioxanes, thioxane, and some other ethers that are difficult to produce via traditional routes could be obtained in 100% selectivity and high yields. In addition, this strategy is also effective for dehydrative etherification of monohydric alcohols, affording various aliphatic ethers and aromatic ethers. A promising H-bond donor-acceptor (D-A) synergistic catalysis mechanism is proposed for the dehydrative etherification of alcohols based on experimental and theoretical studies.

RESULTS

We initiated our investigations by testing the cyclization of 1,5-pentanediol (**1a**) as a benchmark reaction over various ILs, including those with hydrogen bond D-A structures (Table 1 and fig. S1). As shown in Table 1, the ILs with cations having the hydroxyl group (e.g., $[HO\text{-}EtMIm]^+$, $[HO\text{-}EtN_{111}]^+$, and $[HO\text{-}EtMMIm]^+$) and anion $[OTf]^-$ were very effective for transforming **1a** to tetrahydropyran (**1b**), affording **1b** yields in the range of 27 to 91% and **1b** selectivity of 100% at 120°C within 12 hours (entries 1 to 3). However, the other ILs with cations functionalized with -OH group including [HO-EtMIm][BF_4], [HO-EtMIm][PF_6], [HO-EtMIm][NTf_2], [HO-EtMIm][Cl], [HO-EtMIm][OTs], [HO-EtMIm][$N(CN)_2$], [HO-EtMIm][ClO_4], and [HO-EtMIm][NO_3] displayed no activity, and [EtMIm][OTf] was not active for the reaction, although its anion is $[OTf]^-$ (entries 4 to 12). The above results suggest that the synergistic effect between the cation and anion of the effective ILs is the key to catalyzing the reaction.

The acid catalysis mechanism is widely accepted for alcohol dehydration to ethers (*33*). The above effective ILs are weakly acidic, showing much lower acidity compared to commonly used Brønsted acid, such as H_2SO_4. Our experiment showed that the pK_a(H_2O) value of [HO-EtMIm][OTf] is around 4.69. To get evidence for revealing the catalytic mechanism of IL catalysis, we studied the performance of Brønsted acid H_2SO_4 [22 weight % (wt %) aqueous solution, which is generally used in industry], acetic acid, and acidic IL [HO-EtMIm][HSO_4]. In contrast, [HO-EtMIm][OTf] even showed higher activity than H_2SO_4, while acetic acid displayed no activity and [HO-EtMIm][HSO_4] had a little activity (Table 1, entries 1 and 13 to 15). These control experiments suggest that the acid catalysis mechanism is not dominant in the dehydration of **1a** catalyzed by the ILs used in this work.

Using [HO-EtMIm][OTf] as the catalyst, the effects of molar ratios of IL to **1a**, temperature, and reaction time on the cyclization of **1a** were investigated (tables S1 to S3). It was demonstrated that the **1b** selectivity was 100% under all the tested conditions. The IL could serve as both solvent and catalyst, displaying activity in a wide range of molar ratios of IL to **1a**. Notably, 83% yield of **1b** was obtained even at IL loading of 5 mole percent (mol %) (table S1). The reaction could occur at 90°C, and the **1b** yield increased with temperature up to 100% at 130°C (table S2). The reactions initially occurred rapidly, and the yield of **1b** almost increased linearly within 4 hours, achieving ~100% at 15 hours (table S3). In all cases, the reactions occurred in the IL-based phase, and the generated **1b** was spontaneously separated to form a new phase because of its immiscibility with the IL (figs. S2 and S3), thus promoting the reaction efficiently. [HO-EtMIm][OTf] could be easily recovered via simple phase separation and distillation to remove the generated water. The IL could be reused without any loss in activity after five recycles (fig. S4), suggesting its high stability under the experimental conditions (fig. S5) (*30*, *34*). Thus, the [HO-EtMIm][OTf] catalyst shows a superior waste balance with economy factors (E-factors; that is the mass ratio of waste/isolated product) down to 0.40, indicating that this method has promising application potential (*35*, *36*). In addition, scaled-up cyclization of **1a** (10 g) was carried out with [HO-EtMIm][OTf] loading of 10 mol %, and 7.8 g of **1b** was obtained (table S3).

On the basis of the above experimental results, we applied [HO-EtMIm][OTf] in catalyzing cyclization of a series of diols under the optimal conditions, and various O-heterocycles including tetrahydrofurans, tetrahydropyrans, morpholines, dioxanes, and 1,4-thioxane were obtained in high yields without by-products in most cases. As illustrated in Table 2A, a series of five-, six-, and seven-membered

Table 1. IL-catalyzed cyclization of 1,5-pentanediol to tetrahydropyran. Reaction conditions: **1a** (2 mmol); yields were determined by ^{1}H NMR analysis with 1,3,5-trioxane as an internal standard.

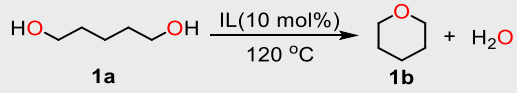

Entry	IL	Yield of 1b
1	[HO-EtMIm][OTf]	91%
2	[HO-EtMMIm][OTf]	27%
3	[HO-EtN_{111}][OTf]	87%
4	[HO-EtMIm][BF_4]	0
5	[HO-EtMIm][PF_6]	0
6	[HO-EtMIm][NTf_2]	0
7	[HO-EtMIm][Cl]	0
8	[HO-EtMIm][OTs]	0
9	[HO-EtMIm][$N(CN)_2$]	0
10	[HO-EtMIm][ClO_4]	0
11	[HO-EtMIm][NO_3]	0
12	[EtMIm][OTf]	0
13	[HO-EtMIm][HSO_4]	5%
14*	H_2SO_4(22 wt %)	61%
15	CH_3COOH	0

*The amount of catalyst was based on H_2SO_4.

Table 2. IL-catalyzed dehydrative etherification of diols and monohydric alcohols to ethers.

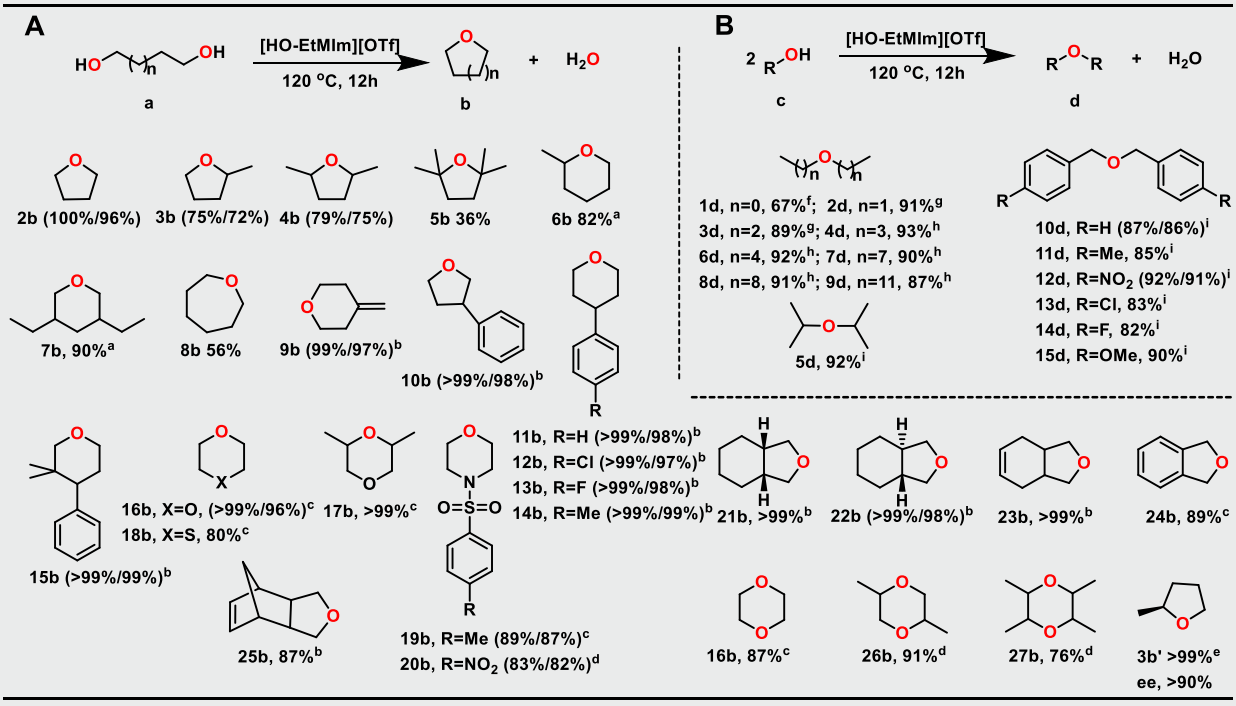

Reaction conditions: (A) alcohol (2 mmol), IL (0.2 mmol): [a]IL (0.4 mmol), 48 hours; [b]IL (1 mmol), 36 hours; [c]IL (1 mmol), 48 hours; [d]IL (1 mmol), 130°C, 48 hours; [e]24 hours. (B) alcohol (2 mmol), IL (1 mmol): [f]alcohol (10 mmol), IL (5 mmol); [g]24 hours; [h]130°C, 24 hours; [i]48 hours. Yields were determined by ^{1}H NMR/isolated yields.

O-heterocycles bearing methyl, dimethyl, ethyl, alkenyl, and phenyl substituted with electron-rich and electron-deficient groups (e.g., methyl, chlorine, and fluorine) were acquired in high yields of 79 to 100% (e.g., **2b**-**4b**, **6b**, and **7b**-**14b**) under the experimental conditions (fig. S6). However, **5b** and **8b** were achieved in low yields of 36 and 56%, respectively, because of the formation of by-products including alkenes and isomerized cyclic ethers (figs. S7 and S8). The diol with a gem-dimethyl group at 3-position (**15a**) was well tolerated, affording product (**15b**) in a yield of 86%. 1,4-Dioxanes (**16b**, **17b**), 1,4-thioxane (**18b**), and osyl-/nosyl-protected morpholines (**19b**, **20b**) that are usually applied in drug design were obtained in high yields from dehydrative etherification of corresponding diols. A series of furans (**21b**-**24b**) were also achieved in 100% selectivity and excellent yields from intramolecular dehydration of corresponding diols (fig. S9). For the diol with two hydroxy groups appended to a carbocyclic ring (**25a**), its intramolecular dehydrative cyclization occurred quickly, producing polycyclic tetrahydrofuran (**25b**), showcasing the potential of this method for the rapid generation of unusual heterocyclic architectures that are of potential interest to drug synthesis (*37*). For the diols with two -OH groups connected on two adjacent C atoms, e.g., ethane-1,2-diol, propane-1,2-diol, and butane-2,3-diol, dehydrative etherification occurred between two diol molecules, forming 1,4-dioxanes (**16b**, **26b**, and **27b**) in high yields without any by-products (fig. S10). Notably, among the above resultant cyclic ethers, **7b**, **12b**-**15b**, **19b**, **20b**, and **26b** were obtained via the dehydrative cyclization of diols.

The IL [HO-EtMIm][OTf] was also effective for catalyzing intermolecularly dehydrative etherification of a wide range of monohydric alcohols, including primary or secondary linear alcohols and benzyl alcohols substituted with electron-donating groups (e.g., -OMe and -Me) and electron-withdrawing groups (e.g., -NO_2, -Cl, and -F), and a series of linear and benzyl ethers were obtained in 100% selectivity and high yields under the experimental conditions (Table 2B, **1d**-**15d**, and fig. S11). However, for some cyclic secondary alcohols such as cyclohexanol and cyclohexyl methyl alcohol, the intermolecular dehydrative etherification occurred to produce ethers (**16d**, **17d**); meanwhile, intramolecular dehydration also took place to generate a considerable amount of olefin by-products (table S4 and figs. S12 and S13), suggesting the strong ability of the IL catalyst for catalyzing the dehydration. In addition, several unsymmetrical ethers could also be obtained in good yields via intermolecularly dehydrative etherification of different alcohols under similar conditions (table S5).

As discussed above, acid catalysis is not the main reaction pathway. To explore the catalytic mechanism of [HO-EtMIm][OTf], the chirality transfer experiment and kinetic studies were performed. As shown in fig. S14A, >99% of (*S*)-2-methyltetrahydrofuran (**3b′**, ee > 90%) was obtained via the dehydrative cyclization of (*R*)-pentane-1,4-diol (**3a′**, ee = 97%), which suggests that the [HO-EtMIm][OTf] catalyst mainly promotes an S_N2 pathway to yield **3b′** and little **3b** may be obtained via an S_N1 pathway under these reaction conditions (*7*, *8*, *38*). Because of the steric effects, the primary alcohol

and secondary carbon acted as the nucleophile and the electrophile, respectively, which resulted in the inversion of configuration for **3a**′ to **3b**′. The rate order of [HO-EtMIm][OTf] was performed by varying its concentrations in the transformation of **1c** to **1d**, and the results indicate that the reaction follows a first-order dependence on catalyst concentrations (figs. S15 and S16). Moreover, an inverse deuterium kinetic isotope effect (k_H/k_D = 0.89) was observed by comparing the rate of dehydrative etherification of **1c** with that of CD_3OH (**1c**′), which supports the idea that the reaction mainly follows an S_N2-like pathway (fig. S14, B and C) (*7*, *9*, *39*). In addition, tertiary alcohol (e.g., **5a**) was also tolerant to this IL catalyst but showed a low reactivity with a 36% yield of **5b** under the similar reaction conditions. This indicates that [HO-EtMIm][OTf] could promote an S_N1 pathway with lower activity in the reaction. Therefore, it can be deduced that both S_N2 and S_N1 pathways may exist simultaneously in the reaction, and [HO-EtMIm][OTf] prefers to promote an S_N2-like pathway.

To further explore the interaction between alcohols and the IL, nuclear magnetic resonance (NMR) experiments were carried out. Because the peaks assigning to O atoms of **1a** and [HO-EtMIm][OTf] in ^{17}O NMR spectra were overlapped, we selected the dehydration of methanol to dimethyl ether (**1d**) as a model reaction to investigate the interaction between alcohol and IL by means of ^1H, ^{17}O, and ^{19}F NMR analyses performed at 60°C (Fig. 2, A and B, and fig. S17). It was demonstrated that the ^1H and ^{17}O NMR spectra of methanol and IL changed considerably as they mixed, indicating the strong interaction between methanol and IL. In the ^1H NMR spectra, the resonance band assigned to the H atom of -OH in $[HO\text{-}EtMIm]^+$ obviously shifted upfield; meanwhile, the resonance band assigned to the O atom of methanol became wider and shifted downfield. These results provide evidence for the formation of the hydrogen bond between the IL cation and methanol molecule in the form of $CH_3\text{-}(H)O\ldots HO\text{-}EtMIm^+$ with the electron transfer from the O atom of methanol to the H atom of -OH in $[HO\text{-}EtMIm]^+$. This indicates that the IL cation serves as a hydrogen-bond donor to form the hydrogen bond with the O atom in methanol, which may activate the C—O bond in methanol.

It is known that both electronegative F and O atoms in [OTf] anion are good hydrogen-bond acceptors for forming hydrogen bonds with the H atom of -OH in methanol (*23*, *40*–*43*). From the ^{17}O, ^{19}F, and ^1H NMR spectra of methanol, IL, and their mixture, it can be observed that the resonance band assigning to O atoms in $[OTf]^-$ shifted from 163.007 to 162.098 ppm, while the signal to the F atoms in $[OTf]^-$ hardly changed and the resonance band to the H atom of -OH in methanol shifted from 4.762 to 4.070 ppm as methanol mixed with the IL (Fig. 2, A and B, and fig. S17A). These findings suggest that the O atoms in $[OTf]^-$ are the hydrogen-bond acceptor to form the hydrogen bond with methanol in the form of $-CF_3(SO_2)O\ldots H\text{-}OCH_3$, which may activate the O—H bond of methanol. The above NMR analysis indicates that the IL cation (i.e., $[HO\text{-}EtMIm]^+$) and anion ($[OTf]^-$) cooperatively catalyze the dehydration between two methanol molecules to **1d**.

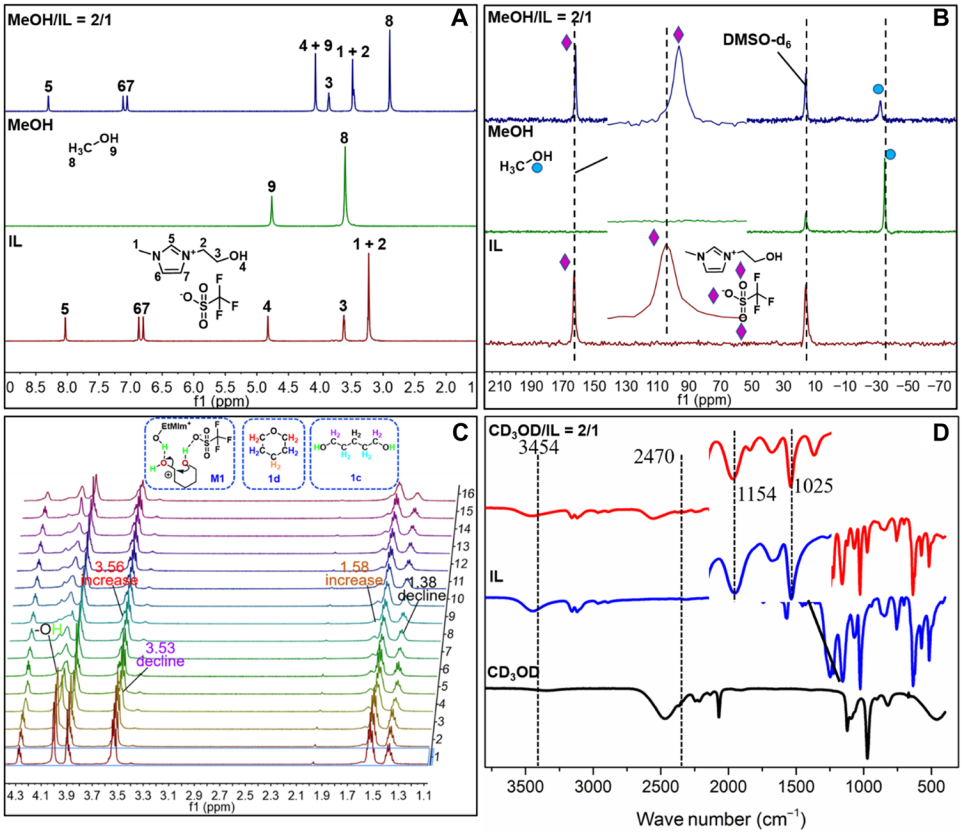

Fig. 2. Mechanistic studies. (**A** and **B**) ^1H and ^{17}O NMR spectra of methanol, IL, and their mixture recorded at 60°C. (**C**) In situ ^1H NMR spectra recorded in **1a** transformation process over [HO-EtMIm][OTf] at 120°C. (**D**) ATR-FTIR spectra of methanol-d_4, IL, and their mixture.

To further explore the catalytic mechanism of [HO-EtMIm][OTf], we performed in situ ^{1}H NMR analysis on **1a** dehydrative etherification over this IL, which provided direct evidence for the strong hydrogen bond interaction between IL and **1a**. As shown in Fig. 2C and fig. S18, the resonance bands of H atoms of -OH in IL and **1a** shifted largely with the corresponding peaks broadening as the reaction proceeded; meanwhile, new peaks appeared in the range of 4.10 to 4.00 ppm in the in situ ^{1}H NMR spectra of the reaction solution of **1a** dehydration over IL, which may be assigned to the H atoms of the intermediate **M1** formed from IL and **1a**. The ^{1}H NMR analysis on **1a**, IL, and their mixture performed at 60°C also supported the above results (fig. S19).

The strong hydrogen bond interaction between methanol and the IL was also evidenced by attenuated total reflection–Fourier transform infrared spectroscopy (ATR-FTIR) spectra (Fig. 2D), in which the characteristic absorption bands for the O—H stretching vibration of IL cation and MeOH-D_4 shifted from 3454 and 2470 cm^{-1} to 3465 and 2564 cm^{-1}, respectively (*43*). Furthermore, the S—O stretching vibration of IL anion slightly shifted from 1026 to 1027 cm^{-1}, which verified the formation of the hydrogen bond between $[OTf]^-$ and MeOH-D_4 (Fig. 2D). In addition, high-resolution electrospray ionization mass spectrometry [HR-ESI-MS(+)] analysis (fig. S20) indicated that the IL could capture methanol molecules to form species like $[(HO\text{-}EtMIm)(CH_3OH)_2]^+$, suggesting the strong interactions between the IL and methanol. Similarly, [HO-EtMIm][OTf] can activate **1a** with the IL cation and anion, respectively, by forming hydrogen bonds with one of the two -OH groups of **1a** in the opposite mode (detailed information was provided in the Supplementary Materials), thus further catalyzing the dehydrative cyclization between the two -OH groups of **1a** to generate **1b**. The above NMR, ATR-FTIR, and ESI-MS(+) analyses indicate that strong hydrogen bond interactions exist between ionic species and alcohol molecules, which realize the activation of C—O and O—H bonds in alcohols, resulting in the dehydrative etherification of alcohols.

Density functional theory (DFT) calculations were performed to gain insight into the hydrogen bonding between **1a** and IL (Fig. 3). For comparison purposes, three ILs— [HO-EtMIm][OTf], [HO-EtN_{111}][OTf], and [HO-EtMIm][Cl]—were selected to perform the DFT calculations (Fig. 3, A to C). From the optimized chemical structures of each IL with **1a**, the distances of hydrogen bond formed between the H atom of -OH in cation and the O atom of **1a** were estimated to be 1.82 Å for [HO-EtMIm][OTf], 1.86 Å for [HO-EtN_{111}][OTf], and 1.81 Å for [HO-EtMIm][Cl], while the distances of hydrogen bonds formed between the O or Cl atom of anion and the H atom of -OH from **1a** were calculated to be 1.90, 1.88, and 2.15 Å for [HO-EtMIm][OTf], [HO-EtN_{111}][OTf], and [HO-EtMIm][Cl], respectively. These results indicate that as a hydrogen-bond donor, the cations (e.g., $[HO\text{-}EtMIm]^+$ and $[HO\text{-}EtN_{111}]^+$) have the similar ability to form very strong hydrogen bonds with **1a**, while as a hydrogen-bond acceptor, $[OTf]^-$ has a much stronger ability to form a hydrogen bond with **1a** than $[Cl]^-$. This can explain why [HO-EtMIm][Cl] was ineffective for the reaction. The calculated corresponding bond energies are consistent with the estimated hydrogen-bond distance results. From the above experimental and calculation results, it can be concluded that both hydrogen bonds of IL cation and anion with alcohol molecules should be strong enough to cooperatively catalyze the dehydration of alcohol.

Figure 3D shows the electrostatic potential (ESP) distribution of [HO-EtMIm][OTf] with **1a**. It is clear that at the areas where the hydrogen bonds are formed, the negative surface potential (blue area) of O in **1a** overlaps with the positive surface potential (red area) of

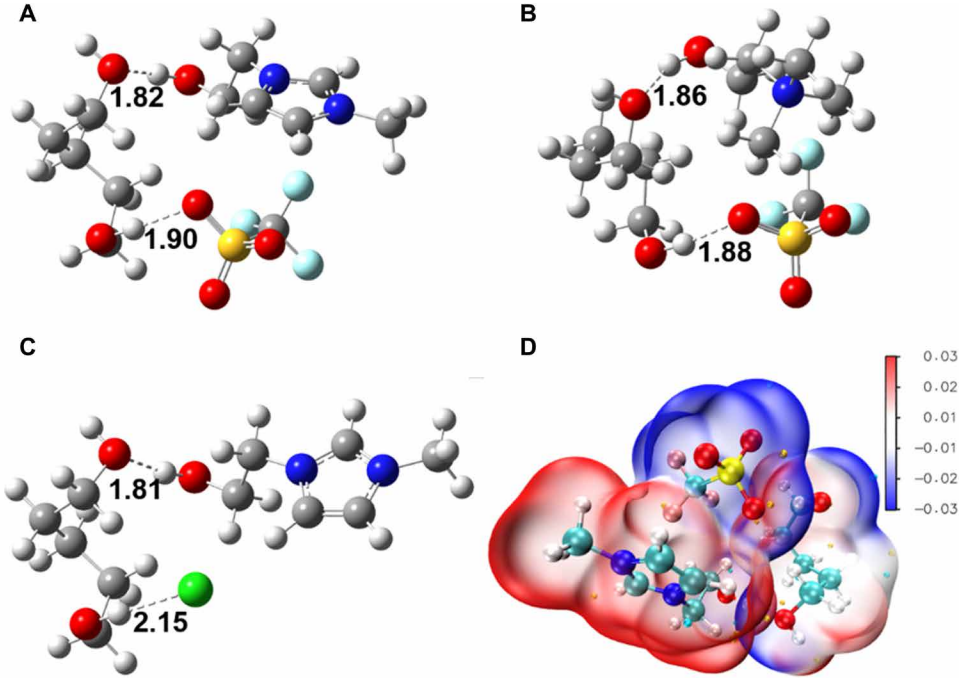

Fig. 3. DFT calculations. (**A** to **C**) Structures of **1a** interacting with [HO-EtMIm][OTf], [HO-EtN_{111}][OTf], and [HO-EtMIm][Cl] optimized at M062X-D3/def2-TZVP level, on which the hydrogen bond distances [black word: atom distance (Å)] are marked. (**D**) Electrostatic potential (ESP) distribution of [HO-EtMIm][OTf] with **1a**.

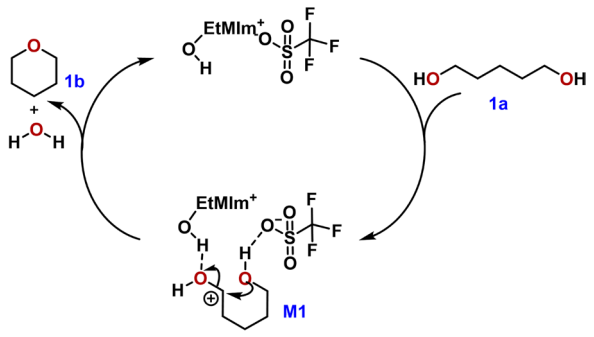

Fig. 4. Proposed reaction pathway of 1a dehydrative cyclization to 1b.

O—H in $[HO\text{-}EtMIm]^+$; meanwhile, the negative surface potential of O in $[OTf]^-$ overlaps with the positive surface potential of O—H in **1a**. This indicates the electrostatic attraction of hydrogen bonds formed between the IL and **1a** (*44*–*46*).

On the basis of the above experimental and calculation results, the reaction mechanism of dehydrative cyclization of **1a** to **1b** is proposed as illustrated in Fig. 4. First, **1a** is activated simultaneously by a pair of IL cation and anion via strong hydrogen bonds in opposite directions. Subsequently, the O atom of one -OH in **1a** forming H-bond with anion attacks the C atom connecting with another -OH in **1a** forming H-bond with cation, producing **1b** followed by the release of one water molecule and regeneration of the IL. This means that the hydrogen bond D-A of IL cooperatively catalyzes the dehydrative cyclization of **1a** to **1b**. The intermolecular dehydration of methanol to **1d** follows the similar reaction mechanism (figs. S21 and S22).

DISCUSSION

In summary, a promising strategy for the synthesis of ethers is presented on the basis of dehydrative etherification of alcohols under cooperative catalysis of hydrogen bond D-A in ILs (e.g., [HO-EtMIm][OTf]), and various ethers including tetrahydrofurans, tetrahydropyrans, morpholines, dioxanes thioxane, aliphatic ethers, and aromatic ethers can be obtained in high yields and 100% selectivity under mild conditions (e.g., 120°C). In particular, some O-heterocycles that are difficult to get via traditional routes have been obtained from dehydrative cyclization of diols. Notably, the generated ethers can be spontaneously separated from the reaction system because of their immiscibility with the IL catalysts, which makes the product separation and purification easily achieved. Moreover, the IL catalyst is recyclable and reusable without activity loss for a long lifetime. This work opens the way for efficiently transforming alcohols to ethers under metal-free, acid-free, and mild conditions. This hydrogen bond D-A cooperative catalysis strategy may be extended to the other type of dehydration reactions, and related work is underway in our group. Therefore, we believe that this simple, efficient, and green strategy has great potential for application in industry.

MATERIALS AND METHODS

Materials

Hydroxyethyl-3-methyl imidazolium trifluoromethanesulfonate ([HO-EtMIm][OTf], 99%), 1-hydroxyethyl-2,3-dimethyl imidazolium trifluoromethanesulfonate ([HO-EtMMIm][OTf], 99%), 1-hydroxyethyl trimethyl ammonium trifluoromethanesulfonate ($[HO\text{-}EtN_{111}][OTf]$, 99%), 1-hydroxyethyl-3-methyl imidazolium tetrafluoroborate ($[HO\text{-}EtMIm][BF_4]$, 99%), 1-hydroxyethyl-3-methyl imidazolium hexafluorophosphate ($[HO\text{-}EtMIm][PF_6]$, 99%), 1-hydroxyethyl-3-methyl imidazolium bis(trifluoromethylsulfonate) imine ($[HO\text{-}EtMIm][NTf_2]$, 99%), 1-hydroxyethyl-3-methyl imidazolium chloride ([HO-EtMIm][Cl], 99%), 1-butylsulfonate-3-methylimidazolium tosylate ([HO-EtMIm][TsO], 99%), 1-hydroxyethyl-3-methyl limidazolium dicyanamide ($[HO\text{-}EtMIm][N(CN)_2]$, 99%), 1-hydroxyethyl-3-methyl limidazolium perchlorate ($[HO\text{-}EtMIm][ClO_4]$, 99%), 1-hydroxyethyl-3-methyl limidazolium nitrate ($[HO\text{-}EtMIm][NO_3]$, 99%), and 1-hydroxyethyl-3-methyl limidazolium trifluoromethanesulfonate ([EtMIm][OTf], 99%) were provided by Centre of Green Chemistry and Catalysis, Lanzhou Institute of Chemical Physics, Chinese Academy of Sciences, and their chemical structures are shown in fig. S1. 1,5-Pentanediol (98%), 1,4-pentanediol (99%), 2,5-dimethyl-2,5-hexanediol (99%), 1,6-hexanediol (98%), diethylene glycol (99%), ethylene glycol (99%), 1,2-propanediol (99%), 2,3-butanediol (mixture of stereoisomers, 98%), ethanol (99.9%), 1-propanol (99.9%), 1-butanol (99.9%), isopropyl alcohol (>99.5%), 1-pentanol (99%), 1-hexanol (99%), 1-heptanol (99%), 1-octanol (98%), benzyl alcohol (99%), 4-methylbenzyl alcohol (99%+), 4-nitrobenzyl alcohol (98%), 4-chlorobenzyl alcohol (99%), 4-methoxybenzyl alcohol (98%), chloroform-d [99.8 atomic % (at %) of D], deuterium oxide (99.9 at % of D), and methyl sulfoxide-d_6 (DMSO-d_6, 99.8 at % of D) were purchased from Beijing InnoChem Science and Technology Co. Ltd. 2,5-Hexanediol (mixture of isomers, 98%), 2,4-diethyl-1,5-pentanediol (DL- and meso-mixture, 93%), *N*,*N*-bis(2-hydroxyethyl)-4-methylbenzene-1-sulfonamide (97%), cis-1,2-cyclohexanedimethanol (95%), (1*R*,2*R*)-cyclohexane-1,2-diyldimeth-anol (98%), 5-norbornene-2,3-dimethanol (mixture of endo- and exo-, predominantly endo-isomer, 95%), 1-nonanol (97%), 1-undecanol (99%), and 4-fluorobenzyl alcohol (>98%) were purchased from TCI Shanghai Co. Ltd. Dipropylene glycol (mixture of isomers, 97%+) was purchased from Adamas. Hexane-2,6-diol (98%) was purchased from TRC. Methanol (99.90%) was purchased from Alfa Aesar. Sulfuric acid (98%) was provided by Sinopharm Chemical Reagent Co. Methanol-D_3 (99.5 at % of D) and methanol-D_4 (99.5 at % of D) were purchased from Acros. Eu(hfc)$_3$ {Europium(III) tris[3-(heptafluoropropylhydroxymethylene)-d-camphorate] puriss. p.a., for NMR spectroscopy} was purchased from Sigma-Aldrich. All reagents were used as received without further purification. The alcohol substrates that are not commercially available were synthesized following the reported procedures (*37*, *47*, *48*), which are given in Supplementary Text.

General procedures for dehydrative etherification of methanol

For methanol dehydration to dimethyl ether, all reactions were conducted in a high-pressure reactor (16 ml of inner volume) equipped with a magnetic stirrer. In a typical experiment, [HO-EtMIm][OTf] (5 mmol) and methanol (10 mmol) were sequentially loaded into the reactor and sealed under the nitrogen atmosphere. Subsequently, the reactor was moved to an oil bath of the desired temperature (e.g., 120°C) and stirred for 12 hours. After the reaction, the reactor was cooled down in ice water. The qualitative analysis of products was conducted using a gas chromatography–mass spectrometer (GC-MS) (Agilent 5975C-7890A) and by comparing with authentic samples. The yields of corresponding ethers were quantitatively analyzed by GC and ^{1}H NMR.

General procedures for dehydrative etherification of alcohols except for methanol

All reactions were conducted in a sealed tube (15 ml of inner volume) equipped with a magnetic stirrer. In a typical experiment, [HO-EtMIm][OTf] (0.2 mmol) and 1,5-pentanediol (2 mmol) were sequentially added into the reactor and sealed under the nitrogen atmosphere. Subsequently, the reactor was moved to an oil bath of desired temperature (e.g., 120°C) and stirred for desired time. After the reaction, the reactor was cooled down in ice water. For NMR analysis, 1,3,5-trioxane (0.0450 g) as an internal standard and $CHCl_3$ (1.5 ml) were added into the reaction mixture. After being stirred vigorously and followed by centrifugation, the lower layer liquid (products) and the IL phase were collected, respectively. The qualitative analysis of the products was conducted using a GC-MS (Agilent 5975C-7890A) and by comparing with authentic samples. The yields of corresponding ethers were quantitatively analyzed by ^{1}H NMR using 1,3,5-trioxane as an internal standard.

The yields of the reactions were calculated on the basis of the following equations

Moles of the product obtained = Moles of the internal standard × Peak area of the corresponding product obtained × The H number of corresponding product obtained/(Peak area of the internal standard × 6)

$$\text{Yield of product} = \frac{\text{Moles of the product obtained}}{\text{Theoretic moles of the product}} \times 100\%$$

Recycling of catalyst

The reusability of the IL [HO-EtMIm][OTf] was tested using the benchmark reaction of **1a** dehydrative cyclization. After the reaction, the reaction mixture in the reactor was transferred into a centrifuge tube. After centrifugation, the IL phase was collected by phase separation and distilled under vacuum to remove the generated H_2O. Then, [HO-EtMIm][OTf] was reused directly for the next run.

pK_a measurements

[HO-EtMIm][OTf] aqueous solution (0.1 M) was prepared, and the pH was measured with a pH meter. Then, pK_a (where K_a is the acid dissociation constant) was calculated on the basis of the following equations

$$\text{pH} = -\lg[\text{H}^+]$$

$$\text{p}K_a = \text{pH} + \lg([\text{HA}]/[\text{H}^+])$$

NMR measurements

NMR spectra were recorded on a Bruker Avance III 400 HD or 500 WB spectrometer equipped with 5-mm pulsed-field gradient probes. Chemical shifts are given in parts per million (ppm) relative to tetramethylsilane. To eliminate the effect of solvent, Wilmad coaxial insert NMR tubes were used for ^{1}H, ^{19}F, ^{17}O, and ^{13}C NMR analysis at 333.2 K. DMSO-d_6 was added in the inner tube, and the sample was added in the outer tube.

For ^{1}H, ^{19}F, and ^{17}O NMR analysis, pure MeOH, [HO-EtMIm][OTf], and the mixture of MeOH and [HO-EtMIm][OTf] with a molar ratio of 2:1 were prepared. Each sample (0.3 ml) was added into the outer tube, and the inner tube was inserted.

For in situ ^{1}H NMR analysis, the mixture of 1,5-pentanediol and [HO-EtMIm][OTf] with a molar ratio of 1:1 was prepared. The mixture (0.5 ml) was added into the NMR tube, and the spectra were recorded every 60 s from 0 to 3 hours at 393.2 K. Sixteen representative in situ ^{1}H NMR spectra were selected to analyze the intermediates during the reaction. For ^{1}H NMR analysis, spectra of **3b** or **3b′** with Eu(hfc)$_3$ (chiral lanthanide shift reagent) were recorded on a Bruker Neo 700 NMR spectrometer equipped with a CP BBO BB-H&F-D 05 probe at 298.2 K.

ATR-FTIR characterization

Pure methanol-d_4, [HO-EtMIm][OTf], and the mixture of methanol-d_4 and [HO-EtMIm][OTf] with a molar ratio of 2:1 were prepared before analysis. FTIR spectra of the liquid samples were detected in the ATR mode on a Bruker Vertex 70 infrared spectrometer at a 1-cm^{-1} resolution. A total of 64 scans were collected for both the background (the air) and the samples.

X-ray diffraction analysis

X-ray intensities were measured on an XtaLAB AFC10 (RCD3): fixed-chi single diffractometer. The crystal was kept at 170.00(10) K during data collection. Intensity data were integrated with the Olex2 software (*49*). The structure was solved with the ShelXT (*50*) structure solution program using intrinsic phasing and refined with the ShelXL (*51*) refinement package using least squares minimization.

HR-ESI-MS characterization

The mixture of methanol (2 ml) and [HO-EtMIm][OTf] (2 mmol) was stirred at room temperature for 12 hours. After stirring, the mixture was analyzed by Bruker FT-ICR-MS (Solarix 9.4T). The ionization method and mode of detection used were indicated for the corresponding experiment, and all masses were reported in atomic units per elementary charge (mass/charge ratio) with an intensity normalized to the most intense peak.

LC-MS characterization

The liquid chromatography–MS (LC-MS) analysis was carried out using LC-MS2010 equipped with a C18 column (Ascentis Express, 2.1 mm × 100 mm × 1.7 μm particle size, Supelco). Mobile phase A was an aqueous solution of formic acid (0.1 wt %), and mobile phase B was an acetonitrile solution of formic acid (0.1 wt %). The flow rate was 0.2 ml/min (gradient program: 90% A and 10% B for 5 min, to 20% A and 80% B for 12 min, to 90% A and 10% B for 2 min, and held for 1 min). Positive ion model was used.

DFT calculations

All calculations were performed with the Gaussian 09 package (*52*). Geometry optimizations were carried out at the M06-2X (*53*)/def2-TZVP (*54*) level at 393.15 K. The frequency calculations were carried out at the M06-2X/def2-TZVP level using the optimized structures to confirm that the reactant and product have no imaginary frequencies and that the transition states (TSs) have only one imaginary frequency. The intrinsic reaction coordinate calculations were used to verify these TSs. Solvation corrections (*55*, *56*) were calculated by a self-consistent reaction field using the SMD-GIL model.

SUPPLEMENTARY MATERIALS

Supplementary material for this article is available at http://advances.sciencemag.org/cgi/content/full/7/22/eabg0396/DC1

REFERENCES AND NOTES

1. J. Xiang, M. Shang, Y. Kawamata, H. Lundberg, S. H. Reisberg, M. Chen, P. Mykhailiuk, G. Beutner, M. R. Collins, A. Davies, M. Del Bel, G. M. Gallego, J. E. Spangler, J. Starr, S. Yang, D. G. Blackmond, P. S. Baran, Hindered dialkyl ether synthesis with electrogenerated carbocations. *Nature* **573**, 398–402 (2019).
2. Q. W. Zhang, A. T. Brusoe, V. Mascitti, K. D. Hesp, D. C. Blakemore, J. T. Kohrt, J. F. Hartwig, Fluorodecarboxylation for the synthesis of trifluoromethyl aryl ethers. *Angew. Chem. Int. Ed.* **55**, 9758–9762 (2016).
3. T. H. Fleisch, A. Basu, R. A. Sills, Introduction and advancement of a new clean global fuel: The status of DME developments in China and beyond. *J. Nat. Gas Sci. Eng.* **9**, 94–107 (2012).
4. Q. Xu, H. Xie, P. Chen, L. Yu, J. Chen, X. Hu, Organohalide-catalyzed dehydrative O-alkylation between alcohols: A facile etherification method for aliphatic ether synthesis. *Green Chem.* **17**, 2774–2779 (2015).
5. R.-Z. Li, D.-Q. Liu, D. Niu, Asymmetric *O*-propargylation of secondary aliphatic alcohols. *Nat. Catal.* **3**, 672–680 (2020).
6. R. H. Beddoe, K. G. Andrews, V. Magné, J. D. Cuthbertson, J. Saska, A. L. Shannon-Little, S. E. Shanahan, H. F. Sneddon, R. M. Denton, Redox-neutral organocatalytic Mitsunobu reactions. *Science* **365**, 910–914 (2019).
7. A. Bunrit, P. Srifa, T. Rukkijakan, C. Dahlstrand, G. Huang, S. Biswas, R. A. Watile, J. S. M. Samec, H_3PO_2-Catalyzed intramolecular stereospecific substitution of the hydroxyl group in enantioenriched secondary alcohols by N-, O-, and S-centered nucleophiles to generate heterocycles. *ACS Catal.* **10**, 1344–1352 (2020).
8. A. Bunrit, C. Dahlstrand, S. K. Olsson, P. Srifa, G. Huang, A. Orthaber, P. J. R. Sjöberg, S. Biswas, F. Himo, J. S. M. Samec, Brønsted acid-catalyzed intramolecular nucleophilic substitution of the hydroxyl group in stereogenic alcohols with chirality transfer. *J. Am. Chem. Soc.* **137**, 4646–4649 (2015).
9. R. A. Watile, A. Bunrit, J. Margalef, S. Akkarasamiyo, R. Ayub, E. Lagerspets, S. Biswas, T. Repo, J. S. M. Samec, Intramolecular substitutions of secondary and tertiary alcohols with chirality transfer by an iron(III) catalyst. *Nat. Commun.* **10**, 3826 (2019).
10. A. R. Bayguzina, L. I. Gimaletdinova, R. I. Khusnutdinov, Synthesis of cyclic ethers from diols in the presence of copper catalysts. *Russ. J. Org. Chem.* **53**, 1840–1843 (2017).
11. G. Gonzalez Miera, A. Bermejo Lopez, E. Martinez-Castro, P. O. Norrby, B. Martin-Matute, Nonclassical mechanism in the cyclodehydration of diols catalyzed by a bifunctional iridium complex. *Chem. A Eur. J.* **25**, 2631–2636 (2019).
12. L. Zhang, A. Gonzalez-de-Castro, C. Chen, F. Li, S. Xi, L. Xu, J. Xiao, Iron-catalyzed cross etherification of alcohols to form unsymmetrical benzyl ethers. *Mol. Catal.* **433**, 62–67 (2017).
13. Y. Yang, Z. Ye, X. Zhang, Y. Zhou, X. Ma, H. Cao, H. Li, L. Yu, Q. Xu, Efficient dehydrative alkylation of thiols with alcohols catalyzed by alkyl halides. *Org. Biomol. Chem.* **15**, 9638–9642 (2017).
14. Y. Li, C. Topf, X. Cui, K. Junge, M. Beller, Lewis acid promoted ruthenium(II)-catalyzed etherifications by selective hydrogenation of carboxylic acids/esters. *Angew. Chem. Int. Ed.* **54**, 5196–5200 (2015).
15. P. Kostetskyy, N. A. Zervoudis, G. Mpourmpakis, Carboranes: The strongest Brønsted acids in alcohol dehydration. *Catal. Sci. Technol.* **7**, 2001–2011 (2017).
16. V. Barbarossa, R. Viscardi, G. Maestri, R. Maggi, D. Mirabile Gattia, E. Paris, Sulfonated catalysts for methanol dehydration to dimethyl ether (DME). *Mater. Res. Bull.* **113**, 64–69 (2019).
17. M. Kang, J. F. DeWilde, A. Bhan, Kinetics and mechanism of alcohol dehydration on γ-Al_2O_3: Effects of carbon chain length and substitution. *ACS Catal.* **5**, 602–612 (2015).
18. D. Masih, S. Rohani, J. N. Kondo, T. Tatsumi, Low-temperature methanol dehydration to dimethyl ether over various small-pore zeolites. *Appl. Catal. Environ.* **217**, 247–255 (2017).
19. T. Mitsudome, T. Matsuno, S. Sueoka, T. Mizugaki, K. Jitsukawa, K. Kaneda, Direct synthesis of unsymmetrical ethers from alcohols catalyzed by titanium cation-exchanged montmorillonite. *Green Chem.* **14**, 610–613 (2012).
20. J. Zhang, P. Chen, B. Yuan, W. Ji, Z. Cheng, X. Qiu, Real-space identification of intermolecular bonding with atomic force microscopy. *Science* **342**, 611–614 (2013).
21. W. Yuan, H. Yang, C. Duan, X. Cao, J. Zhang, H. Xu, N. Sun, Y. Tao, W. Huang, Molecular configuration fixation with C–H···F hydrogen bonding for thermally activated delayed fluorescence acceleration. *Chem* **6**, 1998–2008 (2020).
22. E. V. Beletskiy, J. Schmidt, X. B. Wang, S. R. Kass, Three hydrogen bond donor catalysts: Oxyanion hole mimics and transition state analogues. *J. Am. Chem. Soc.* **134**, 18534–18537 (2012).
23. J. L. Jeffrey, J. A. Terrett, D. W. MacMillan, O–H hydrogen bonding promotes H-atom transfer from α C–H bonds for C-alkylation of alcohols. *Science* **349**, 1532–1536 (2015).
24. O. Coulembier, D. P. Sanders, A. Nelson, A. N. Hollenbeck, H. W. Horn, J. E. Rice, M. Fujiwara, P. Dubois, J. L. Hedrick, Hydrogen-bonding catalysts based on fluorinated alcohol derivatives for living polymerization. *Angew. Chem. Int. Ed.* **48**, 5170–5173 (2009).
25. H. Zhang, S. Lin, E. N. Jacobsen, Enantioselective selenocyclization via dynamic kinetic resolution of seleniranium ions by hydrogen-bond donor catalysts. *J. Am. Chem. Soc.* **136**, 16485–16488 (2014).
26. K. Dong, S. Zhang, Q. Wang, A new class of ion-ion interaction: Z-bond. *Sci. China Chem.* **58**, 495–500 (2015).
27. J. Reichenbach, S. A. Ruddell, M. Gonzalez-Jimenez, J. Lemes, D. A. Turton, D. J. France, K. Wynne, Phonon-like hydrogen-bond modes in protic ionic liquids. *J. Am. Chem. Soc.* **139**, 7160–7163 (2017).
28. L. Hao, Y. Zhao, B. Yu, Z. Yang, H. Zhang, B. Han, X. Gao, Z. Liu, Imidazolium-based ionic liquids catalyzed formylation of amines using carbon dioxide and phenylsilane at room temperature. *ACS Catal.* **5**, 4989–4993 (2015).
29. M. Liu, Z. Zhang, H. Liu, Z. Xie, Q. Mei, B. Han, Transformation of alcohols to esters promoted by hydrogen bonds using oxygen as the oxidant under metal-free conditions. *Sci. Adv.* **4**, eaas9319 (2018).
30. H. Wang, Y. Zhao, F. Zhang, Y. Wu, R. Li, J. Xiang, Z. Wang, B. Han, Z. Liu, Hydrogen-bonding catalyzed ring-closing C-O/C-O metathesis of aliphatic ethers over ionic liquid under metal-free conditions. *Angew. Chem. Int. Ed.* **59**, 11850–11855 (2020).
31. K. Chen, G. Shi, W. Zhang, H. Li, C. Wang, Computer-assisted design of ionic liquids for efficient synthesis of 3(2H)-furanones: A domino reaction triggered by CO_2. *J. Am. Chem. Soc.* **138**, 14198–14201 (2016).
32. J. Hu, J. Ma, Q. Zhu, Z. Zhang, C. Wu, B. Han, Transformation of atmospheric CO_2 catalyzed by protic ionic liquids: Efficient synthesis of 2-oxazolidinones. *Angew. Chem. Int. Ed.* **54**, 5399–5403 (2015).
33. W. Alharbi, E. F. Kozhevnikova, I. V. Kozhevnikov, Dehydration of methanol to dimethyl ether over heteropoly acid catalysts: The relationship between reaction rate and catalyst acid strength. *ACS Catal.* **5**, 7186–7193 (2015).
34. H. Wang, Y. Zhao, Z. Ke, B. Yu, R. Li, Y. Wu, Z. Wang, J. Han, Z. Liu, Synthesis of renewable acetic acid from CO_2 and lignin over an ionic liquid-based catalytic system. *Chem. Commun.* **55**, 3069–3072 (2019).
35. P. H. Huy, S. Motsch, S. M. Kappler, Formamides as lewis base catalysts in SN reactions-efficient transformation of alcohols into Chlorides, Amines, and Ethers. *Angew. Chem. Int. Ed.* **55**, 10145–10149 (2016).
36. M. Sheykhan, Z. Rashidi Ranjbar, A. Morsali, A. Heydari, Minimisation of E-Factor in the synthesis of *N*-hydroxylamines: The role of silver(I)-based coordination polymers. *Green Chem.* **14**, 1971–1978 (2012).
37. T. Biberger, S. Makai, Z. Lian, B. Morandi, Iron-catalyzed ring-closing C-O/C-O metathesis of aliphatic ethers. *Angew. Chem. Int. Ed.* **57**, 6940–6944 (2018).
38. P. T. Marcyk, L. R. Jefferies, D. I. AbuSalim, M. Pink, M.-H. Baik, S. P. Cook, Stereoinversion of unactivated alcohols by tethered sulfonamides. *Angew. Chem. Int. Ed.* **131**, 1741–1745 (2019).
39. C. Kohlmeyer, A. Schäfer, P. H. Huy, G. Hilt, Formamide-catalyzed nucleophilic substitutions: Mechanistic insight and rationalization of catalytic activity. *ACS Catal.* **10**, 11567–11577 (2020).
40. T. Min, J. C. Fettinger, A. K. Franz, Enantiocontrol with a hydrogen-bond directing pyrrolidinylsilanol catalyst. *ACS Catal.* **2**, 1661–1666 (2012).
41. S. M. Banik, A. Levina, A. M. Hyde, E. N. Jacobsen, Lewis acid enhancement by hydrogen-bond donors for asymmetric catalysis. *Science* **358**, 761–764 (2017).
42. P. A. Champagne, Y. Benhassine, J. Desroches, J. F. Paquin, Friedel-Crafts reaction of benzyl fluorides: Selective activation of C-F bonds as enabled by hydrogen bonding. *Angew. Chem. Int. Ed.* **53**, 13835–13839 (2014).
43. T. Bauer, M. Voggenreiter, T. Xu, T. Wähler, F. Agel, K. Pohako-Esko, P. Schulz, T. Döpper, A. Görling, S. Polarz, P. Wasserscheid, J. Libuda, ZnO nanoparticle formation from the molecular precursor $[MeZnO^tBu]_4$ by Ozone treatment in ionic liquids: In-situ vibrational spectroscopy in an ultrahigh vacuum environment. *Z. Anorg. Chem.* **643**, 31–40 (2017).
44. T. Lu, F. Chen, Multiwfn: A multifunctional wavefunction analyzer. *J. Comput. Chem.* **33**, 580–592 (2012).
45. J. Zhang, LIBRETA: Computerized optimization and code synthesis for electron repulsion integral evaluation. *J. Chem. Theory Comput.* **14**, 572–587 (2018).
46. S. Wu, W. Zhang, L. Qi, Y. Ren, H. Ma, Investigation on 4-amino-5-substituent-1, 2, 4-triazole-3-thione Schiff bases an antifungal drug by characterization (spectroscopic, XRD), biological activities, molecular docking studies and electrostatic potential (ESP). *J. Mol. Struct.* **1197**, 171–182 (2019).
47. C. K. Steinhardt, Private communication, in *Reagents for Organic Synthesis*, L. F. Fieser, M. Fieser, Eds. (John Wiley & Sons, 1967), vol. 1, p. 584.
48. N. Ríos-Lombardía, V. Gotor-Fernández, V. Gotor, Complementary lipase-mediated desymmetrization processes of 3-aryl-1,5-disubstituted fragments. Enantiopure synthetic valuable carboxylic acid derivatives. *J. Org. Chem.* **76**, 811–819 (2011).

49. O. V. Dolomanov, L. J. Bourhis, R. J. Gildea, J. A. Howard, H. Puschmann, *OLEX2*: A complete structure solution, refinement and analysis program. *J. Appl. Cryst.* **42**, 339–341 (2009).
50. N. K. Sebbar, M. Ellouz, E. M. Essassi, Y. Ouzidan, J. T. Mague, Crystal structure of 4-benzyl-2H-benzo[b][1,4]thiazin-3(4H)-one. *Acta Crystallogr.* **71**, o999 (2015).
51. G. M. Sheldrick, SHELXT—Integrated space-group and crystal-structure determination. *Acta Crystallogr.* **71**, 3–8 (2015).
52. Gaussian 09, Revision D.01, M. J. Frisch, Wallingford, CT (2009).
53. Y. Zhao, D. G. Truhlar, The M06 suite of density functionals for main group thermochemistry, thermochemical kinetics, noncovalent interactions, excited states, and transition elements: Two new functionals and systematic testing of four M06-class functionals and 12 other functionals. *Theor. Chem. Acc.* **120**, 215–241 (2008).
54. F. Weigend, R. Ahlrichs, Balanced basis sets of split valence, triple zeta valence and quadruple zeta valence quality for H to Rn: Design and assessment of accuracy. *Phys. Chem. Chem. Phys.* **7**, 3297–3305 (2005).
55. A. V. Marenich, C. J. Cramer, D. G. Truhlar, Universal solvation model based on solute electron density and on a continuum model of the solvent defined by the bulk dielectric constant and atomic surface tensions. *J. Phys. Chem. B* **113**, 6378–6396 (2009).
56. V. S. Bernales, A. V. Marenich, R. Contreras, C. J. Cramer, D. G. Truhlar, Quantum mechanical continuum solvation models for ionic liquids. *J. Phys. Chem. B* **116**, 9122–9129 (2012).
57. J. C. Killen, L. C. Axford, S. E. Newberry, T. J. Simpson, C. L. Willis, Convergent syntheses of 3,6-Dihydroxydec-4-enolides. *Org. Lett.* **14**, 4194–4197 (2012).
58. E. Keinan, K. K. Seth, R. Lamed, Organic synthesis with enzymes. 3. TBADH-catalyzed reduction of chloro ketones. Total synthesis of (+)-(S,S)-(cis-6-methyltetrahydropyran-2-yl)acetic acid: A civet constituent. *J. Am. Chem. Soc.* **108**, 3474–3480 (1986).
59. A. Greb, J. S. Poh, S. Greed, C. Battilocchio, P. Pasau, D. C. Blakemore, S. V. Ley, A versatile route to unstable diazo compounds via oxadiazolines and their use in Aryl–Alkyl cross-coupling reactions. *Angew. Chem. Int. Ed.* **56**, 16602–16605 (2017).
60. F. Zhang, D. Zheng, L. Lai, J. Cheng, J. Sun, J. Wu, Synthesis of aromatic sulfonamides through a copper-catalyzed coupling of aryldiazonium tetrafluoroborates, DABCO·$(SO_2)_2$, and *N*-chloroamines. *Org. Lett.* **20**, 1167–1170 (2018).
61. T. Ohta, T. Miyake, N. Seido, H. Kumobayashi, H. Takaya, Asymmetric hydrogenation of olefins with aprotic oxygen functionalities catalyzed by BINAP-Ru (II) complexes. *J. Org. Chem.* **60**, 357–363 (1995).

Acknowledgments

Funding: This work was supported financially by the National Natural Science Foundation of China (21890761, 21533011, and 21773266) and the Chinese Academy of Sciences (QYZDY-SSW-SLH013-2). **Author contributions:** H.W. and Z.L. designed the project and prepared the manuscript for publication. H.W. and Y.Z. carried out the experiments and collected the data. F.Z. and H.W. performed the calculations. All authors analyzed the data and contributed to the writing of the manuscript. **Competing interests:** Z.L., H.W., Y.Z., and B.H. are inventors on a patent application related to this work filed by National Intellectual Property Administration, P.R. China (nos. 202011221942.4, 202011222685.6, and 202011222719.1, filed on 5 November 2020). The authors declare no other competing interests. **Data and materials availability:** All data needed to evaluate the conclusions in the paper are present in the paper and/or the Supplementary Materials. Additional data related to this paper may be requested from the authors.

Submitted 7 December 2020
Accepted 6 April 2021
Published 26 May 2021
10.1126/sciadv.abg0396

Citation: H. Wang, Y. Zhao, F. Zhang, Z. Ke, B. Han, J. Xiang, Z. Wang, Z. Liu, Hydrogen-bond donor and acceptor cooperative catalysis strategy for cyclic dehydration of diols to access O-heterocycles. *Sci. Adv.* **7**, eabg0396 (2021).